Scientific Research Publishing

World Journal of Nuclear Science and Technology, 2022, 12, 69-87
https://www.scirp.org/journal/wjnst
ISSN Online: 2161-6809
ISSN Print: 2161-6795

Pseudocritical Rapid Energy Dissipation Analysis of Base-Load Electrical Demand Reduction on Nuclear Steam Supply System

Frederick Agyemang[1], Stephen Yamoah[1,2], Seth Kofi Debrah[1,2]

[1]Graduate School of Nuclear and Allied Science, University of Ghana, Accra, Ghana
[2]Nuclear Power Institute, Ghana Atomic Energy Commission, Accra, Ghana
Email: fagyemang007@st.ug.edu.gh, s.yamoah@gaecgh.org, s.debrah@gaecgh.org

How to cite this paper: Agyemang, F., Yamoah, S. and Debrah, S.K. (2022) Pseudocritical Rapid Energy Dissipation Analysis of Base-Load Electrical Demand Reduction on Nuclear Steam Supply System. *World Journal of Nuclear Science and Technology*, **12**, 69-87.
https://doi.org/10.4236/wjnst.2022.122007

Received: February 2, 2022
Accepted: April 24, 2022
Published: April 27, 2022

Abstract

Effect of pseudocritical rapid energy dissipation (PRED) from Pressurizer in nuclear steam supply system of Pressurized Water Reactor, where a single event as common cause failure, of considerable reduction of base-load electricity demand causes the temperature of the reactor coolant system (RCS) to increase, and corresponding pressure increases in pressurizer and steam generators above set-points. The study employed the uses of MATLAB/Simulink library tools, to experimentally modelled pressure control as PRED, where the momentum of transport of kinematic viscosity fraction above pseudocritical point dissipated as excess energy, to maintain the safety of the Pressurizer and RCS and keep the water from boiling. The result demonstrated the significance of pressure vector and Prandlt number as heat transfer coefficients that provided detailed activities in 2-D contour and 3-D graphics of specific internal energy and other parameterization of fluid in the pressurizer.

Keywords

Pseudocritical Rapid Energy Dissipation, Pseudocritical Saturation, Parameterization, Internal Energy, Pressure Vector, Heat Transfer Coefficient

1. Introduction

A considerable reduction of base-load electricity demand generated by nuclear power plant (NPP) for industrial and domestic applications, classified as common cause failure (CCF), may cause the temperature of the reactor coolant to increase and corresponding pressure increase in Pressurizer and Steam Generators. The short fall in terms of electricity demand triggers an integrated plant

control system (IPCS) of nuclear instrumentation and control (I & C) systems into action, to compensate for the demand reduction of the base-load, since the amount of heat released from the nuclear chain reaction must be proportional to the amount of heat taking away for generation of electrical energy.

The Pressurizer in NPP maintains the pressure of reactor coolant system (RCS), preserves the threshold parameters through the steady state operations, and regulates the pressure during the transient process of the Reactor. The Pressurizer pressure control system (PPCS) forms part of the IPCS of the nuclear steam supply system (NSSS) of the Pressurized Water Reactor (PWR) [1]. It offers three main functions: 1) to protect the reactor from trip, 2) to protect the reactor from changes in reactivity and 3) to protect the activation of pressure relief valve [2]. The introduction of Pseudocritical rapid energy dissipation (PRED) pressure control, seeks to maintain the safety of the Pressurizer and the RCS.

The Pressurizer operates on three main functions that take place concurrently; 1) the dynamics of temperature variation, 2) the rise and fall of pressure values and 3) the variation of water/steam levels. The rod control system regulates the in-core rod position, the power and the power distribution. The input of the pressurizer pressure is the deviation from a set-point, while the output drives proportional spray controller, to actuate heaters and power relief valve within fixed operating points. The other system controllers provide ex-core integrated plant control by synchronization of fluid flow and control signal activities.

Most of the reactors in operation today are about 40 - 50 years older. The assessment of existing Instrumentation and control (I & C) systems, and its modernization needs in terms of obsolete systems and the impact of failure rate, the NSSS-I & C appeared to be of high priority for modernization [3], the NSSS has reach its operational limits and condition (OLC). The nuclear I & C system serves as nerve center of NPP [4], to coordinate activities of thousands of components and equipment [5], that allow the plant operators to monitor the safe operation of NPP. The advances made by the evolution of digital technology have improved operations of automation and control systems, and yet the nuclear industry remains conservative with the use of analogue systems, hence the need for the proposed modern PRED I & C system.

The level control of pressurizer represent balance of injection of water inflow into the reactor coolant system and water letdown into the chemical and volume control system (CVCS) [6]. The two-phase simulation model of compressibility involving the thermodynamic equilibrium revealed sub-critical evaporation with large variation of liquid compressibility factor and density [7].

A two-phase turbulence model where interfacial turbulence accounts for pseudoturbulence in liquid bubble-induced mixing [8]. The hyperbolic transition model of two-phase fast depressurization is highlighted on six equations of two-phase model, for accurate tabulation of equation of state (EoS) for thermodynamic equilibrium recovery, for depressurization of water-steam system [9]. Which referred to PWR with water as coolant with highly non-linear behavior of two-phase,

model provided thermodynamic separation between water and steam independent of each other.

Modern instrumentation and control system was used to examine the effect heat transfer of fluid properties, MATLAB/Simulink library tools was used to: 1) design a model of pseudocritical rapid energy dissipation I & C system, where thermophysical properties of the two-phase fluid characteristics with introduction of three thermodynamic property sensors. Analyze pseudocritical saturation line, the effect of specific internal energy, pressure vector and other parameterization of fluid content of Pressurizer. Evaluated the effect of heat transfer coefficient (Prandtl number) and momentum of the transport of the kinematic viscosity, as pseudocritical rapid energy dissipation from pressurizer.

2. Theories

The pressurizer relief line connect the pressurizer safety and relief valve to the pressurizer relief tank with the input coming from refueling water and storage tank.

The energy conservation in the pressurizer sometimes referred to in the study as pipe or open-channel can be expressed as [10].

$$M\bar{u}_I + \left(\dot{m}_A + \dot{m}_B\right)u_I = \phi_A + \phi_B + Q_H \tag{1}$$

where, M is the fluid mass inside the pressurizer, $\dot{m}_A$ and $\dot{m}_B$ are the mass flow rate into the pipe through port A and B, while u_I is the specific internal energy of the fluid inside the pressurizer, ϕ_A is the energy flow rate into the pressurizer through port A. While ϕ_B is the energy flow rate into the pressurizer through port B, and Q_H is the heat flow rate into the pressurizer through the pressurizer wall represented by port subscript $_{\mathrm{H}}$ is the thermal conductive insulator.

The energy conservation in the pressurizer is given by the energy balance equation as expressed in "Equation (2)" [11]:

$$P_A - P_I = \frac{\dot{m}_A}{S}\left|\frac{\dot{m}_A}{S}\left(V_I - V_A\right)\right| + F_{visc,A} + I_A \tag{2}$$

where: P_A is the pressure at port A, S is the cross-sectional area of the pressurizer, V_A is the specific volume of the fluid at port A, $F_{visc,A}$ is the viscous friction force is port A, I_A is the fluid inertia at port A which is further expressed as in "Equation (3)",

$$I_A = \dot{m}_A \frac{L}{2S} \tag{3}$$

where L is the length of the pressurizer in the half pipe adjacent to port B.

Similarly, for port B, the energy conservation in the pressurizer can be expressed as,

$$P_B - P_I = \frac{\dot{m}_B}{S}\left|\frac{\dot{m}_A}{S}\left(V_I - V_B\right)\right| + F_{visc,B} + I_B \tag{4}$$

The heat flow rate inside the walls of the pressurizer and the internal fluid volume was modelled as

$$Q_H = h_{coeff} S_{surf} \left(T_H - T_I \right) \tag{5}$$

where, h_{coeff} is the average heat transfer coefficient, S_{surf} is the surface area, T_H is the pressurizer wall temperature and T_I is the temperature of the fluid in the pressurizer.

The heat transfer coefficient rely on the phase of the fluid. With subcooled liquid and superheated vapour conditions, [12] the coefficient was modelled as:

$$h_{coeff}^{*} = \frac{k_I^{*} Nu^{*}}{D_h} \tag{6}$$

The asterisk represent a value of the phase under consideration (liquid or vapour). While N_u is the average Nusselt number in the pipe, k_I is the average thermal conductivity in the pressurizer, and D_h is the hydraulic diameter.

$$h_{coeff}^{M} = \frac{k_{I,SL}^{M} Nu^{M}}{D_h} \tag{7}$$

The subscript ^{M} refers to specific value of two-phase mixture and $_{SL}$ is the saturated liquid.

The Nusselt number have effect on convective and conductive heat transfer coefficient, for laminar flow assumed as constant, while the Reynolds number acts on the inertia and viscous forces applied when the value is smaller than the laminar flow [13].

The Gnielinski correlation [14], expressed in "Equation (8)" was used to compute the Nusselt number in the liquid and vapour phases:

$$Nu^{*} = \frac{\frac{f}{8}\left(Re^{*} - 1000 \right) Pr_I^{*}}{1 + 12.7\sqrt{\frac{f}{8}}\left(Pr_I^{*2/3} - 1 \right)} \tag{8}$$

where, f is the friction factor of the pressurizer, Re is the Reynolds number and Pr_I is the Prandtl number.

The friction factor was evaluated as:

$$f = \left\{ -1.8 \log_{10} \left[\frac{6.9}{Re^{*}} + \left(\frac{\varepsilon_r}{3.7} \right)^{1.11} \right] \right\}^{-2} \tag{9}$$

where, ε_r is the roughness of the pressurizer inner walls. The Reynolds number was expressed as:

$$Re^{*} = \frac{\left| \dot{m}_{Avg} \right| D_h v_I^{*}}{S v_I^{*}} \tag{10}$$

where the subscript $_{Avg}$ represent an average value between the ports, S is the cross-sectional area, v_I is the specific volume and v_I is the kinematic viscosity.

For the two-phase mixture, the Nusselt number for turbulent flow correlation expressed by Cavallini and Zecchin [15] was utilized as in "Equation (11)".

$$Nu^{M} = 0.05\left[\left(1 - x_I + x_I\sqrt{\frac{v_{SV}}{v_{SL}}}\right)Re_{SL}\right]^{0.8} Pr_{SL}^{0.33} \tag{11}$$

where subscript $_{SL}$ represent the saturated liquid and $_{SV}$ saturated vapor, x_I is the vapour quality and v is the specific volume.

The Reynolds number of the saturated liquid is expressed as

$$Re_{SL} = \frac{\left|\dot{m}_{Avg}\right| D_h v_{SL}}{S v_{SL}} \tag{12}$$

The conservation of mass balance in the pressurizer was modelled according to Equation (13)

$$\left[\left(\frac{\delta\rho}{\delta\rho}\right)_u \dot{p}_I + \left(\frac{\delta\rho}{\delta u}\right)_p \bar{u}_I\right] V = \dot{m}_A + \dot{m}_B + \varepsilon_M \tag{13}$$

where, ρ is the fluid density, $\dot{p}_I$ is the pressure inside the pressurizer, V is the volume of fluid, $\dot{m}_A$ is the mass flow rate into the pipe through port A, $\dot{m}_B$ is the mass flow rate into the pipe through port B and ε_M is the correction term density partial derivation of transition phase boundaries.

The density partial derivative using cubic polynomial function of subcooled blended with superheated vapour in two-phase mixture domain was accounted for according to "Equation (14)".

$$\varepsilon_M = \frac{M - V/v_I}{\tau} \tag{14}$$

where the ε_M is the cubic polynomial function introduces the numerical error has always a single inflection point. M is the fluid mass in the pressurizer and is expressed as where v_I as the specific volume of the fluid in the pressurizer, τ is the phase change time constant.

$$\dot{M} = \dot{m}_A + \dot{m}_B \tag{15}$$

In the laminar regime, the Reynolds number limit value in port A was specified by:

$$F_{visc.A}^{laminar} = \frac{f_{shape} L_{eff} v_I \dot{m}_A}{4 D_h^2 S} \tag{16}$$

and the half pipe adjacent to port B by:

$$F_{visc.B}^{laminar} = \frac{f_{shape} L_{eff} v_I \dot{m}_B}{4 D_h^2 S} \tag{17}$$

where, f_{shape} is the pipe shape factor, L_{eff} is the effective pipe length and D_h is the hydraulic diameter of the pipein the turbulent regime, the Reynolds number limit for port A was specified according to "Equation (18)".

$$F_{visc.A}^{turbulent} = \frac{\dot{m}_A \left|\dot{m}_A\right| f_A L_{eff} v_I}{4 D_h^2 S} \tag{18}$$

while in the half pipe adjacent to port B, it was specified as

$$F_{visc.B}^{turbulent} = \frac{\dot{m}_B |\dot{m}_B| f_B L_{eff} v_I}{4 D_h^2 S} \tag{19}$$

In Equations "(18)" and "(19)", f_A is the Darcy friction factor for turbulent flow in the half pipe adjacent to port A and f_B is the Darcy friction factor for turbulent flow in the half pipe adjacent to port B.

The Darcy friction factor [16] for the turbulent to port A was modelled by utilizing Haaland equation for ports A and B as expressed in Equations "(20)" and "(21)" respectively.

$$f_A = \frac{1}{\left\{-1.8 \log_{10}\left[\frac{6.9}{Re_A} + \left(\frac{\varepsilon_r}{3.7}\right)^{1.11}\right]\right\}^{-2}} \tag{20}$$

The half pipe adjacent to port B

$$f_B = \frac{1}{\left\{-1.8 \log_{10}\left[\frac{6.9}{Re_B} + \left(\frac{\varepsilon_r}{3.7}\right)^{1.11}\right]\right\}^{-2}} \tag{21}$$

The Darcy friction factor formulates the friction losses in the pressurizer similar to the losses in pipe flow and other open-channel flow. The Haaland equation explicitly approximates experimental results of laminar and turbulent flow in pipe, open channels or pressurizer.

3. Methods

The pressure control system (Figure 1) sends a signal to the actuator valve, either to open or to shut the valve. The monitoring system compare the output value and apply proportional-integral-derivative (PID) values based on the errors from the feedback values to the summer, which adds the set-point figures to the error values.

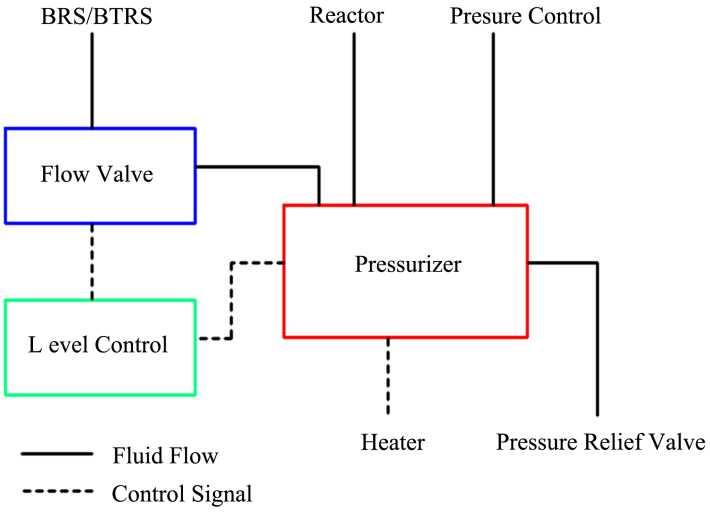

Figure 1. Pressure control system.

The designed model of PRED is based on two-phase fluid domain which consists of elements, sources and sensors linked with fluid within the loop network. The schematic in Figure 2 incorporated three new sensors: 1) pressure & Internal energy sensor, 2) thermodynamic property sensor and 3) two-phase fluid property sensor. In addition, the controlled pressure source also known as pseudocritical rapid dissipation valve (PRDV), a physical signal (P) that control the pressure source and vent out excess energy buildup in the pressurizer in order to restore the transient state to the desire steady state operation set-point values.

The PRED control system designed model consist of two-phase (2P) fluid domain, linked with the fluid within the loop network, fulfilled the requirements for the configuration solver to compiled and initialized the model design, updated the library link blocks, evaluated the block parameters, construct the system equations for the physical network and initialized the design ready for simulation.

The PRED functions involve distinct interactions of the multivariable multiple-input multiple-output (MIMO) system is quite complex. There are 1) solid and liquid, where the liquid chemical content (particles) interact with the solid materials such as the pressurizer walls and the heating elements. 2) Solid and gaseous, here the solid materials of the pressurizer and the piping network (the carriers for steam) interact with the vapour. 3) Liquid and vapour, where the volume of the liquid has one phase and interact with the volume of vapour as the second phase. 4) The Combine internal components within the pressurizer where the chain effect of these interactions and other factors have significant influence on the pressurizer.

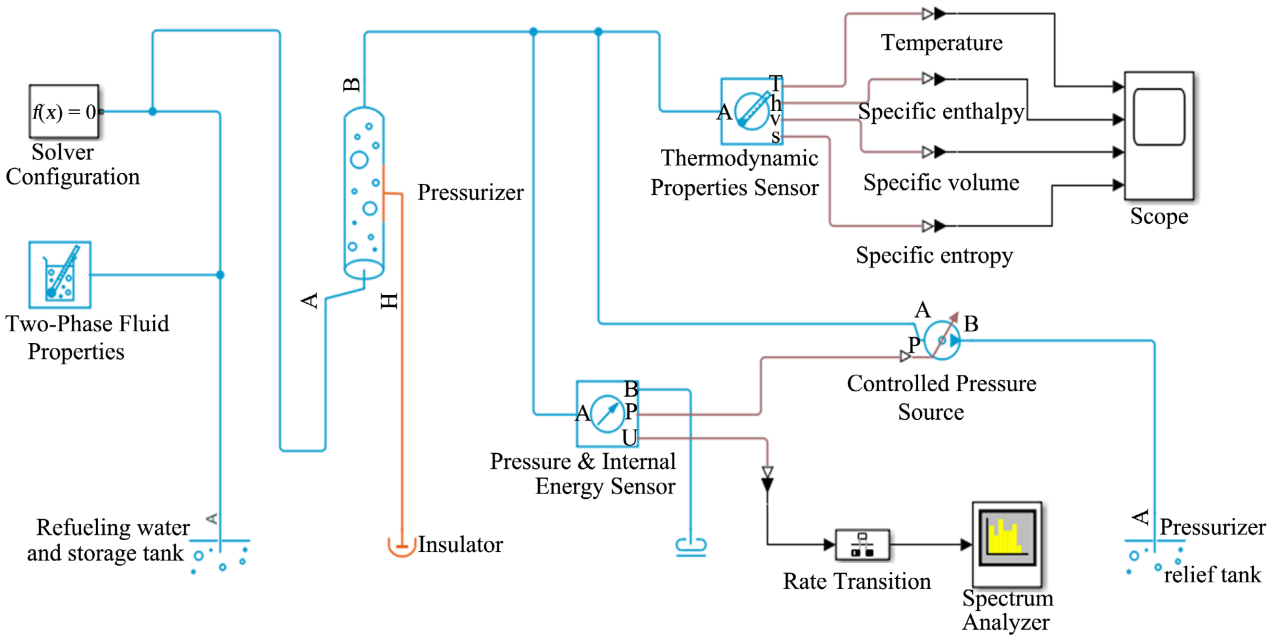

Figure 2. Pseudocritical rapid energy dissipation.

4. Results

The thermodynamic analysis of fluid properties has been widely studied in 1D graphics. However, such representation does not provide detail illustration compared to the 2-D contour and the 3-D graphics. The thermodynamic properties sensor in PRED provided the plot of the magnitude and phase of the temperature, specific enthalpy, specific volume and specific entropy against time at reference zero of the fluid in one-dimensional (1D) display (Figure 3).

The temperature values simulated for 10 seconds appeared to be constant, however, the range of temperature measured in degree Celsius ranges from 280 degree Celsius to 330 degree Celsius for specified time.

The spectrum analyzer plotted the noise power spectral density (Figure 4) that illustrated the peak as finder and distortion measurement of specified number of harmonics with the corresponding power measured in dBm/Hz. The

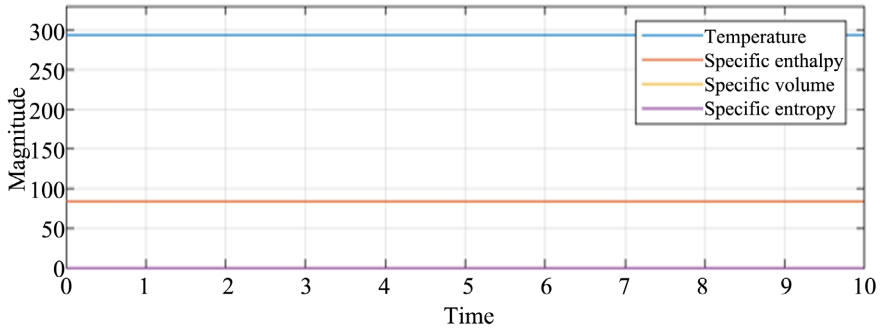

Figure 3. Plot of Thermodynamic properties.

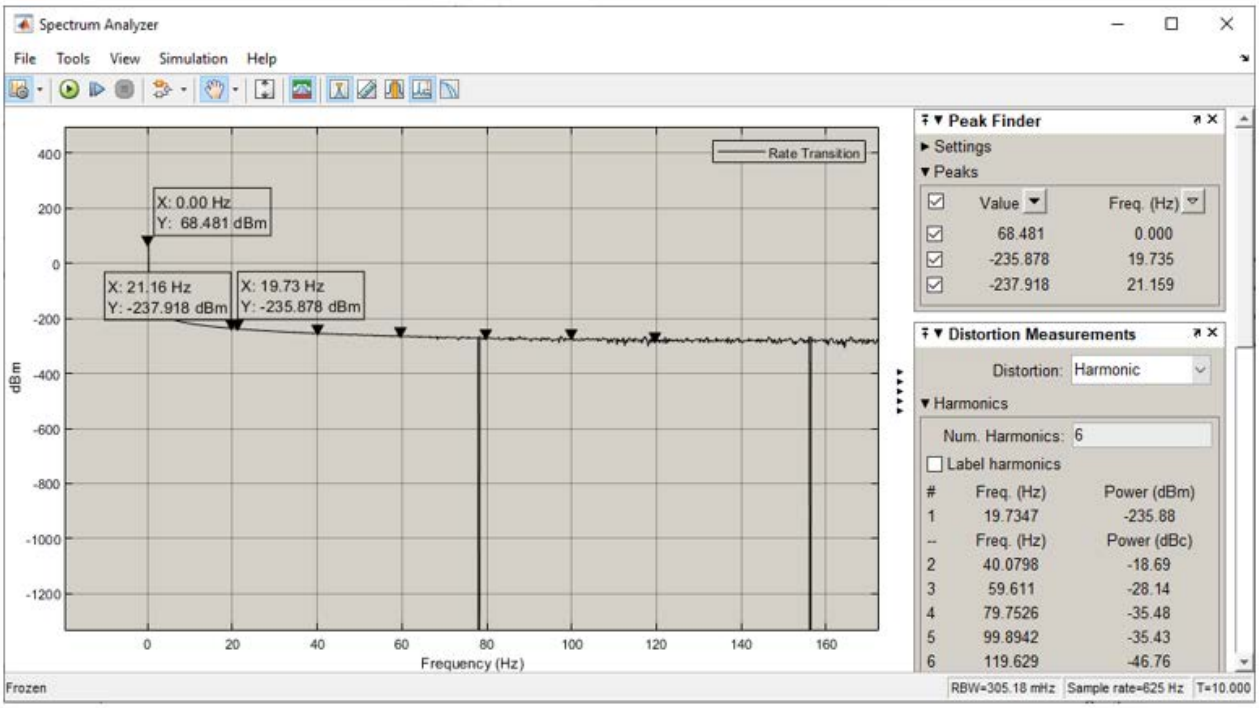

Figure 4. Plot of distortion measurement.

device under test (DUT) was the pressure and internal energy sensor where selected peak finder provided corresponding peak values and frequencies was determined. The Gaussian reference plot provided complementary cumulative distribution function (CCDF), where the average maximum power in decibels was measured.

The Spectrum Analyzer displayed the results of the fundamental frequencies of the total harmonics distortion (THD), where the frequency variation was considered as the sum of the internal energy of the water, the steam produced, the pressure and the volume of fluid within the pressurizer. The distortion measured by six harmonics at different frequencies with different power levels measured in decibels equals −400.38 dBm.

4.1. Effect of Pseudocritical Saturation

The flow dynamics of the two-phase have effect on the fluid inertia, the viscous friction losses and the convective heat transfer within the pressurizer. The volume of the fluid is assumed to be constant, where the pressure and temperature of the fluid affect the thermal conservation of the pressurizer.

The proposed PRED function coordinates activities of the heaters to compensate for the heat loss of the pressurizer to achieve equilibrium between steam and water. The subcooled liquid has normalized internal energy defined as:

$$\bar{u} = \frac{u - u_{\min}}{u_{sat}^{L}(p) - u_{\min}} - 1, \quad u_{\min} \le u < u_{sat}^{L}(p) \tag{22}$$

where, $\bar{u}$ is the normalized internal energy of the fluid, u is the specific internal energy of the fluid, $\bar{u}_{\min}$ is the minimum specific internal energy and $\bar{u}_{sat}^{L}$ is the specific internal energy of the liquid at saturation as shown in Equations "(22)" to "(24)".

The changes in the internal energy of the pressurizer depends on specific volume of the liquid, the temperature and the pressure, due to the energy balance of the chemical reaction (**Figure 5**). The Pressure vector (0.001 and 100) coordinates the pressure values that provided the grid surface points. The pressure of the liquid is within the minimum values, why the pressure above the pseudocritical saturation approaches the maximum value.

At the critical pressure of 172 bar plus 22.0640 bar with atmospheric pressure of 0.101325 bar, where the critical point with saturated liquid internal energy of $x = 2071$ kJ/kg and pressure values of $y = 24.77$ bar (typical value 196.77 bar).

The specific volume (m^3/kg) of the liquid (**Table 1**) represented the pressure vector and internal energy at specific grid point, where the boundary of saturation above or at the critical pressure is equal to vapour specific volume.

At the critical pressure the properties of the water gradually changes from liquid with small compressibility and high density to gaseous with low density and high compressibility. The physical properties of the liquid such as specific enthalpy, specific heat and density also changes with the changing temperatures, resulting in subcooled liquid and superheated steam as shown Equation (6) and Equations "(22)" and "(23)".

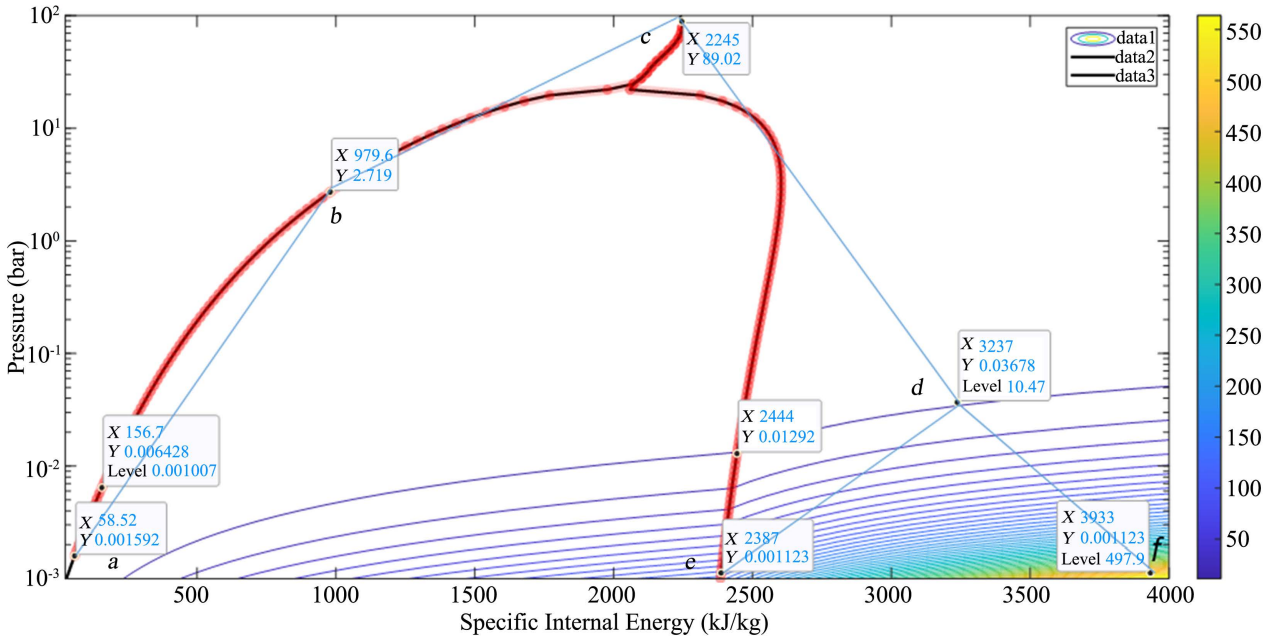

Figure 5. Effect of Pseudocritical saturation on specific volume.

Table 1. Specific volume as variable.

Test Point	*a*	*b*	*c*	*d*	*e*	*f*
Specific Internal energy (kJ/kg), *x*	58.52	979.6	2245	3237	81.5	2402
Pressure Vector (bar), *y*	0.001682	2.179	89.02	0.03678	0.002257	0.002257
Specific volume (m^3/kg), *z*	inf	inf	inf	10.47	inf	497.9

The superheated vapour of the normalized internal energy was expressed as,

$$\bar{u} = \frac{u - u_{\max}}{u_{\max} - u_{sat}^{V}(p)} + 2, \quad u_{sat}^{V}(p) < u \le u_{\max} \tag{23}$$

where, $\bar{u}_{\max}$ is the maximum specific internal energy and $\bar{u}_{sat}^{V}$ is the specific internal energy of saturated vapour.

The specific entropy around the saturation boundary as per unit mass of liquid and vapour at saturation, where the liquid phase and vapour phase changes to mixture state in **Figure 6**.

Where the pressure vector at the upper part of the pressurizer registered 62.8 bar, the base remain at the minimum range with values of 0.001417 bar. While the specific internal energy ranges between 117 and 3933 kJ/kg/K and the specific entropy (kJ/kg/K) registered variable figures at different levels (**Table 2**).

The normalized internal energy of the two-phase mixture was evaluated as defined below:

$$\bar{u} = \frac{u - u_{sat}^{L}(p)}{u_{sat}^{V}(p) - u_{sat}^{L}(p)}, \quad u_{sat}^{L}(p) \le u \le u_{sat}^{V}(p) \tag{24}$$

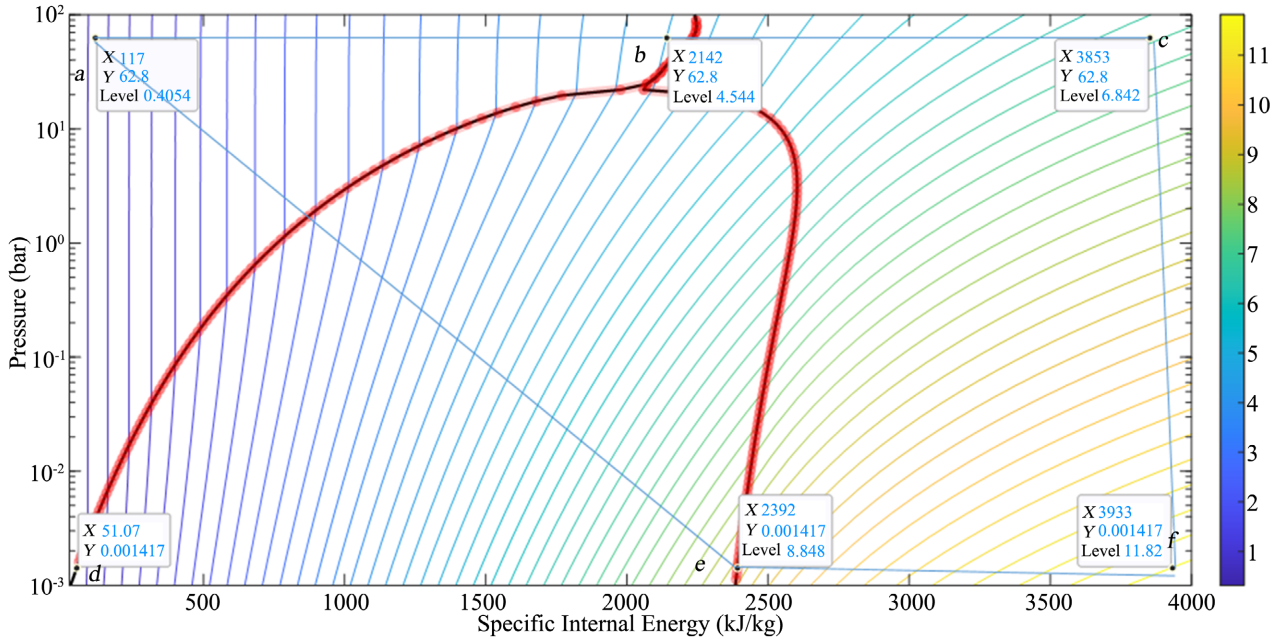

Figure 6. Liquid and vapour mixer state.

Table 2. Internal energy of specific entropy.

Test Point	*a*	*b*	*c*	*d*	*e*	*f*
Specific Internal energy (kJ/kg), *x*	117	2142	3853	51.07	2392	3933
Pressure Vector (bar), *y*	62.8	62.8	62.8	0.001417	0.001417	0.001417
Specific entropy (kJ/kg/K), *z*	0.4054	4.544	6.842	inf	8.848	11.82

For the initial fluid energy set for specific enthalpy with the default value of 1500 kJ/kg for the inertial specific internal energy. Equations "(22) to (24)" as the expression of normalized internal energy at all pressures where the minimum valid specific internal energy is minus one, the liquid saturation boundary is zero, the vapour saturation boundary is plus one, and the maximum valid specific internal energy is plus two.

Where the parameterization of the fluid properties in terms of pressure and normalized internal energy ($\bar{u}$), a linear transformation of specific internal energy (u), as the heat capacity and temperature of the subcooled liquid.

The internal energy axis of temperature in degree Celsius of the different regions of subcooled liquid and superheated vapor in two-phase mixture of saturated specific internal energy and pressure (**Figure 7**).

The Pseudocritical line or the Pseudocritical point is the point when the pressure above the critical pressure and the temperature reaches the maximum value of specific heat at particular pressure.

The interpolation of *x*, *y* and *z* values of the mesh grid where $x = 2071$ kJ/kg, $y = 24.77$ kJ/kg and Thermal conductivity level of 0.4047 mW/m/K represent the

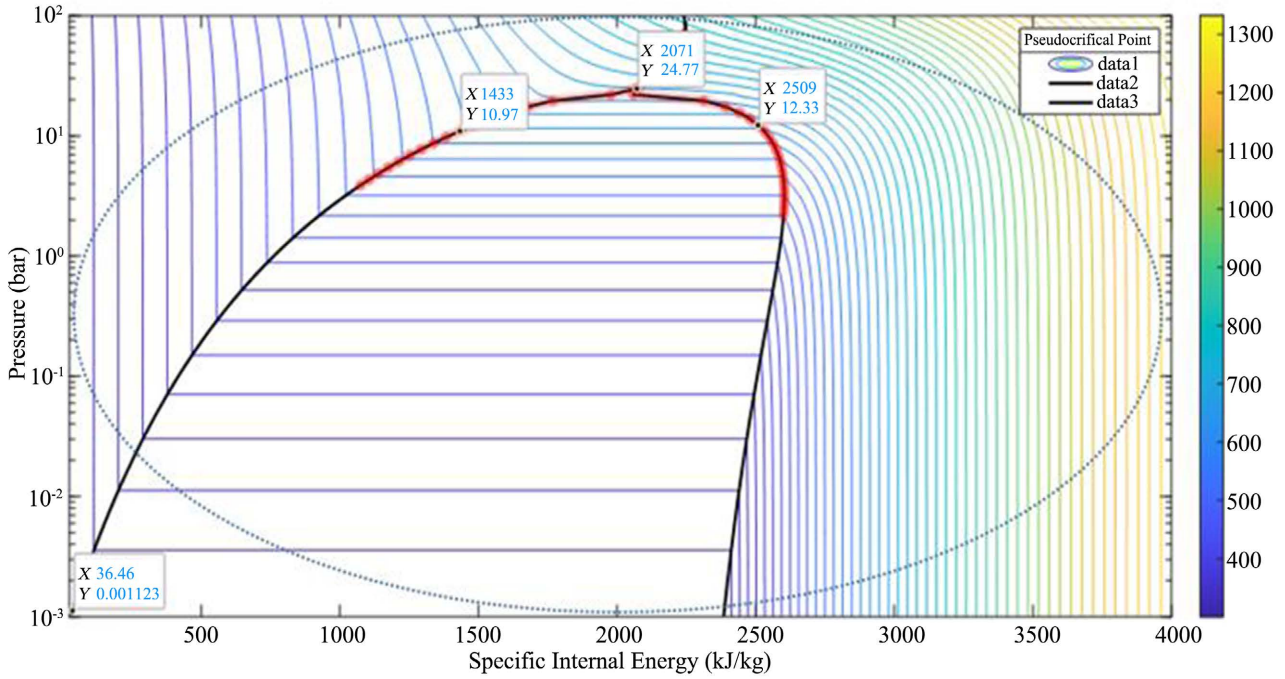

Figure 7. Effect of temperature on internal energy and pressure vector.

pseudocritical point. Where the pressure values at point B and point C is equal to 19.63 bar above the 172 bar, with different specific internal energy values and different Prandtl numbers (Figure 8). Whiles the pressure vector values at points E, F and G with y values equals 0.002257 bars, with variable specific internal energy values.

The contour lines showing specific entropy (kJ/kg/K) that illustrate the dependence of the critical pressure c_p and the critical volume c_v. Where gases was considered to have constant specific heat over a specified range of temperatures.

The Point A serves as the pseudocritical rapid dissipation point (PRDP) where the specific internal energy value of x = 2071 kJ/kg and the pressure value for y = 24.77 bar plus 172 bar. Where the fluid becomes supercritical, the liquid and the vapour ceases to exist separate phases. The boundary between the merger of liquid and vapour represent the pseudocritical line. Where the specific internal energy values at points B, C and D correspond to 533.6; 2594 and 3810 kJ/kg respectively as shown in Table 3.

The liquid Prandtl number provided a table of matrix 25 × 100 that corresponds to pressure vector and normalized internal energy, where the saturated boundary above the critical pressure is clipped. These numerical values of specific internal energy and pressure vector correspond to the point x = 2071 kJ/kg and y = 24.77 bar plus 172 bar as the critical point (Figure 9).

The effect of Prandtl number on laminar flow regime of Newtonian fluid arises due to viscous stress and correlation of local strain overtime, as a heat transfer between the movement of fluid and that of the solid bodies of the pressurizer walls and the heating coil element.

Table 3. Thermal conductivity selected grid points.

Test Point	*A*	*B*	*C*	*D*	*E*	*F*	*G*
Specific Internal energy (kJ/kg)	2071	533.6	2594	3810	81.5	2402	3800
Pressure Vector (bar)	24.77	19.63	19.63	13.85	0.002257	0.002257	0.002257
Thermal Conductivity (mW/m/K)	0.4047	0.6949	0.1057	0.1316	0.5969	0.01805	0.1155

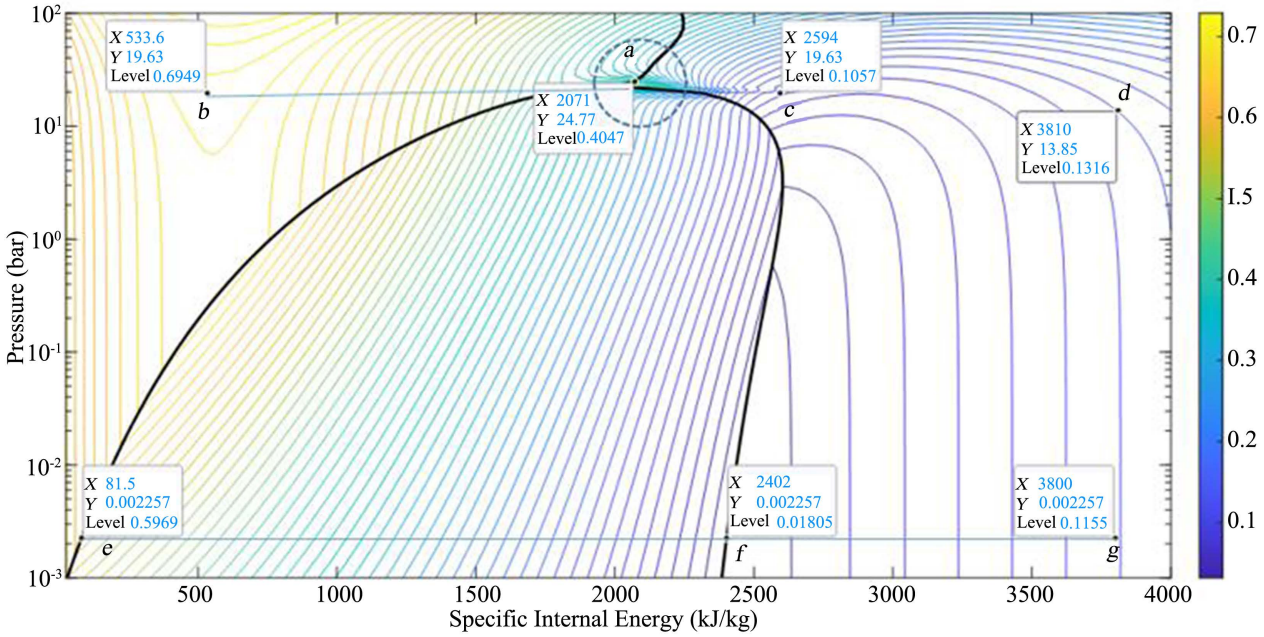

Figure 8. Effect of thermal conductivity on internal energy.

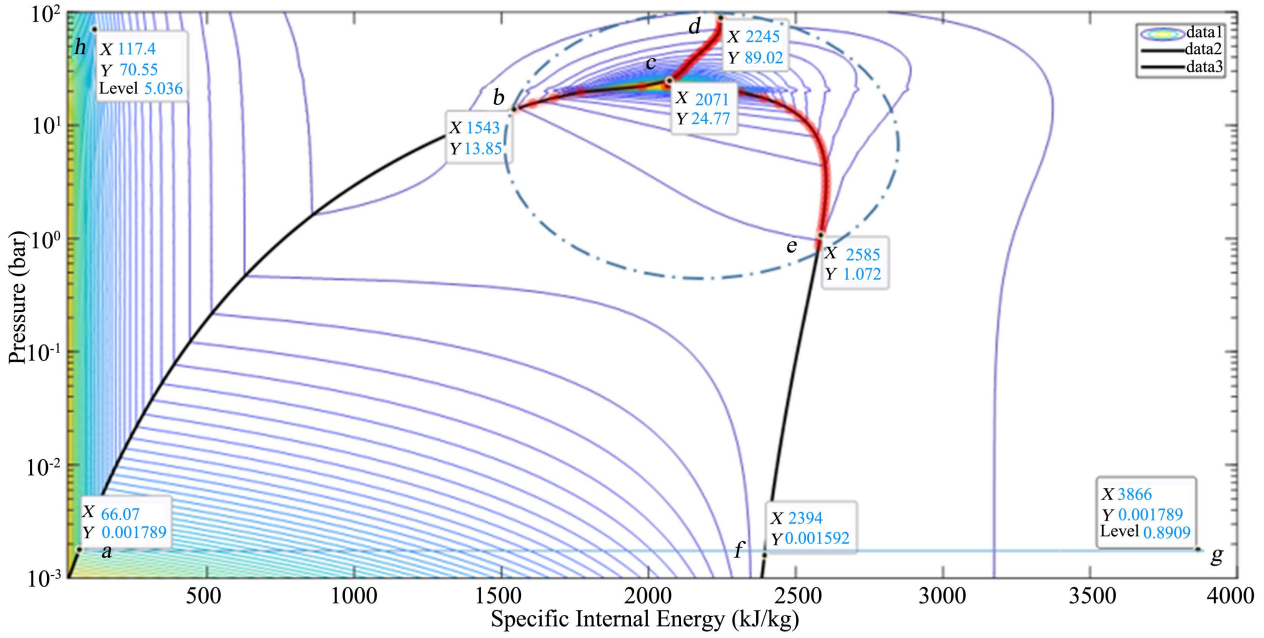

Figure 9. Effect of Prandtl number on specific internal energy.

The Prandtl numbers along the pseudocritical saturation line remain infinity, while the level values at points g = 0.8909 and h = 5.036 dimensionless, with corresponding values of specific internal energy and pressure vector as shown in Table 4 and Table 5.

The resultant manipulations provided graphical illustrations of two dimension (2-D) contours where the pressure above the critical point provided pseudocritical line, the specific internal energy over the supercritical portion of the saturated internal energy critical value, pressure vector and other parameterization.

Effect of Pseudocritical Saturation in 3-D

The dynamics of the system is subject to temperature changes and the mass flow rate of the liquid into the pressurizer and the outlet of vapour from the pressurizer. The internal energy of the gas according to Waal's is not a function of the specific volume. The total change in internal energy depends on the change in volume, temperature and pressure. The energy production in the fluid is due to the rate of change of chemical reaction, where the total energy balance depends on the first law of thermodynamic (energy transport).

Under steady state operation, the specific enthalpy seeks to balance the energy equation in terms of incoming and outgoing variable parameters. These changes include specific volume of the fluid and the pressure of the fluid or vapour, where low enthalpy corresponds to high mass liquid flow rate and high volumetric flow rate. There are other regimes such as supersonic and hypersonic velocity associated with gas flow from pressurizer or steam generator. The thermodynamic propertied of the liquid and vapour differ from each other.

The specific entropy as thermodynamic property, where the default substance (water) used to analyze the entropy per unit mass. The entropy determines the amount of heat transfer used to perform the task of steam generation within the Pressurizer. Here the specific entropy of the two phase as dependent of pressure, temperature and the level of the fluid in the Pressurizer.

The kinematic viscosity at point a remains as low as 0.1276 mm^2/s, that at point e is extremely as high at the value of 26,940 mm^2/s (Table 6). The kinematic

Table 4. Effect of Prandtl number above infinity.

Test Point	a	b	c	d	e	f
Specific Internal energy (kJ/kg)	66.07	1543	2071	2245	2585	2394
Pressure Vector (bar)	0.001789	13.85	24.77	89.02	1.072	0.001592

Table 5. Prandtl number below threshold.

Test Point	g	h
Specific Internal energy (kJ/kg)	3866	117.4
Pressure Vector (bar)	0.001789	70.55
Prandtl number	0.8909	5.036

Table 6. Kinematic viscosity on Pseudocritical line.

Test Point	*a*	*b*	*c*	*d*	*e*
Specific Internal energy (kJ/kg), *x*	2040	2071	36.46	2384	4000
Pressure Vector (bar), *y*	100	24.77	0.001123	0.001	0.001
Kinematic viscosity (mm^2/s), *z*	0.1276	0.1254	1.358	1182	26,940

viscosity of the fluid in the pressurizer is the inherent shear stress to flow, where the kinematic of liquid decreases with temperature and increases with temperature for gasses.

The thermal conductivity of specific liquid depends on the nature of that liquid, where thermal conductivity of water differs from other solid and liquids (**Figure 10**). The thermal conductivity of water changes due to temperature changes that correspond to the changes of atomic vibration frequency of the liquid.

In addition, the analysis of the thermal conductivity of liquid in NSSS pressurizer, where the thermal conductivity (W/m/K) values is a fraction of the thermal properties with the values from points *a* to *e* ranging between 0.4381 to 0.7361 as shown in **Table 7**.

The thermal conductivity of solid and liquids have correlation with the Prandlt number and that of Nusselt number. Depending on the laminar flow, the transitional flow and the turbulent flow, where the effect of pressure is minimal. The increase in temperature of the heater decreases the conductivity of the liquid due to the viscosity of the water, where the correlation of liquid and solid are function of temperature.

The thermal transport properties data provide specific heat, thermal conductivity and the Prandtl number that shows the large peak close to the critical point (**Figure 11**). The two-phase fluid properties offer visual representation of the function of pressure and specific internal energy. The Prandtl number (dimensionless) provided the correlation between viscosity of the fluid and that of the thermal conductivity.

The Prandtl number defines the momentum of the transport of the kinematic viscosity of the liquid as the ratio of the heat transport. At the critical point, the specific internal energy value is 2059 kJ/kg, while the critical pressure is 22.05 + 172 bar and the corresponding Prandlt number is 13.38.

The thermal transport properties of the critical pressure range near the critical point, where the peak value is large or sharp with the width as a fraction, which is either above or below the critical pressure, a region clip at peak values using selective option. A small pressure range around the critical point can be limited by clipping. The action of pseudocritical rapidly energy dissipate from pressurizer indicating the Prandtl number as thermal expansion coefficient, which truncate the effect of excess energy at the critical pressure point and prevent the water of the reactor coolant system from boiling.

Table 7. Thermal conductivity.

Test Point	*a*	*b*	*c*	*d*	*e*
Specific Internal energy (kJ/kg)	25	763.5	1687	2059	29.3
Pressure Vector (bar)	100	100	100	22.05	0.001
Thermal conductivity (W/m/K)	0.6271	0.7361	0.5338	0.4381	0.5722

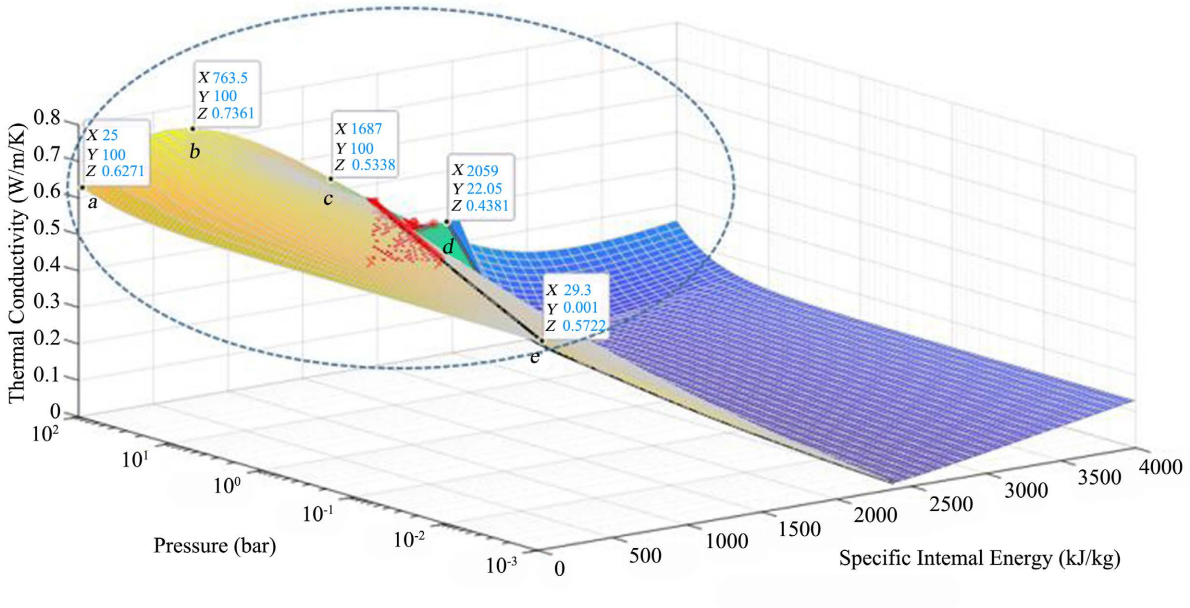

Figure 10. Effect of transport thermal conductivity.

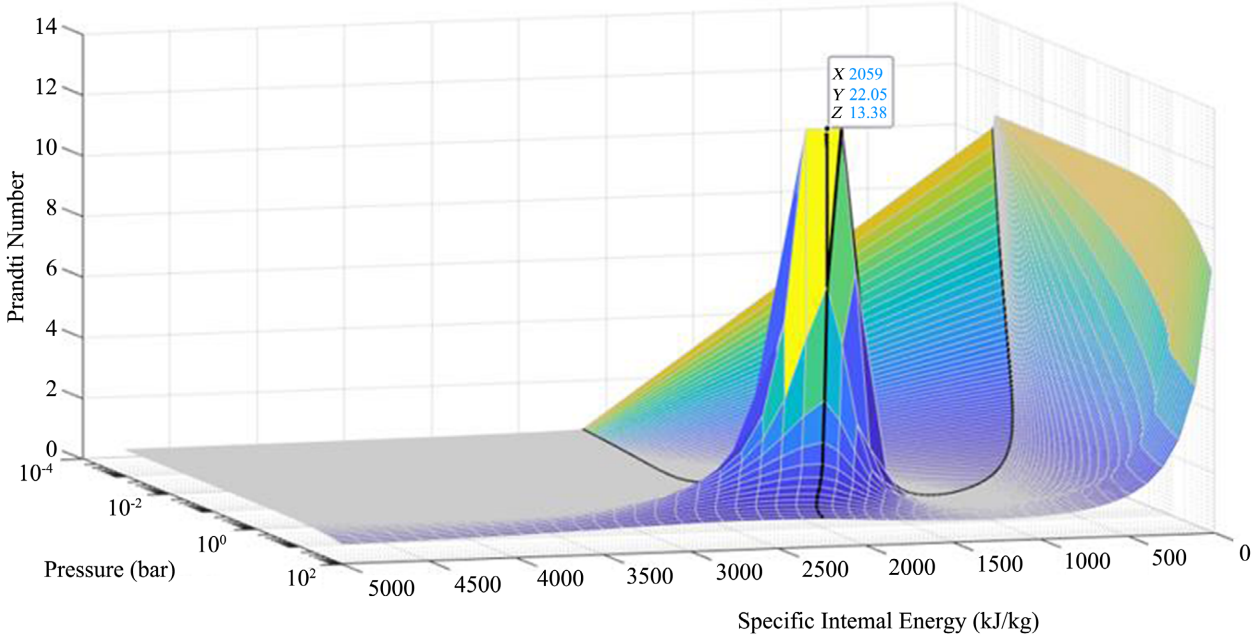

Figure 11. Pseudocritical rapid energy dissipation from Pressurizer.

5. Conclusions

The "Pseudocritical rapid energy dissipation (PRED) from Pressurizer in Nuclear steam supply system", the study affirmed the significance of heat transfer coefficient between conductive and convective heat transfer with the Nusselt number as the ratio of convective heat transfer and conductive heat transfer. The Reynolds number provided the thermal diffusion as the ratio of the inertia forces to the viscous forces. While the Prandtl number offered the ratio of momentum diffusivity and the diffusivity boundaries layers in 2-D contour and 3-D illustrations.

The additional data provided from the lookup table for the parameterization of Density, Isothermal bulk modulus, Isobaric thermal expansion coefficient, Specific internal energy, Specific heat at constant pressure, Kinematic viscosity and Thermal conductivity plotted against Temperature, Pressure and specific internal energy with heat transfer coefficient (Prandtl) and pressure vector as correlation variables.

The thermodynamic properties of two-phase fluid characteristics change into subcooled liquid and superheated steam. At the boundaries when the fluid becomes supercritical as the liquid and the vapour ceases to exist in separate phases, where the merger of the liquid and vapour is the point of pseudocritical saturation, the liquid becomes subcooled and the vapour tends to be superheated.

The action of the controlled pressure source acting as the rapid dissipation control valve provided the Pseudocritical Rapid Energy Dissipation from the Pressurizer, the corresponding effect restores the system pressure back to the threshold values. Where the proportional heaters are energized and provide block of heat that changes the water into steam to reestablish the set-point values, for the safety of the Pressurizer as it maintains the reactor coolant system and keeps the water from boiling even at high temperatures.

Recommendation for future works in 2-D and 3-D Pressurizer level control, where the Boron Recycle System (BRS) and the Boron Thermal Regeneration System (BTRS) forms part of the nuclear steam supply system, parameters that determine the chemical concentration of boron and offers a balance in terms of chemical and volume control system (CVCS).

Acknowledgements

The data provided by the lookup table imbedded in Matlab/Simulink/Simscape (Acknowledgement 1994-2019 The MathWorks, Inc. ARPACK, Copyright © 2001, Rice University. Developed by D.C. Sorensen, R.B. Lehoucq, C. Yang, and K. Maschhoff). All rights reversed.

Conflicts of Interest

The authors declare no conflicts of interest regarding the publication of this paper.

References

[1] Testa, D. and Kunkle, A. (1984) The Westinghouse Pressurized Water Reactor Nuclear Power Plant. Westinghouse Electric Corporation Water Reactor Divisions, 41-47.

[2] Ma, J., Chan, A. and Lv, L. (2012) Mathematical Modeling and Simulation of Pressurizer Pressure Control System. *The 2nd International Conference on Computer Application and System Modeling*, Paris, 2012, 362-366. https://doi.org/10.2991/iccasm.2012.91

[3] IAEA (2004) Managing Modernization of Nuclear Power Plant Instrumentation and Control Systems IAEA. Vienna, 2004.

[4] IAEA (2011) Core Knowledge on Instrumentation and Control Systems in Nuclear Power Plants. IAEA Nuclear Energy Series Publications, Vienna.

[5] IAEA (2018) Approaches for Overall Instrumentation and Control Architectures of Nuclear Power Plants. IAEA Nuclear Energy Series No. NP-T-2.11 Vienna, Austria.

[6] Zhang, G.-D., Yang, X.-H., Ye, X.-L., Xu, H., Lu, D.-Q. and Chen, W. (2012) Research on Pressurizer Water Level Control of Pressurized Water Reactor Nuclear Power Station. *Energy Procedia*, **16**, 849-855. https://doi.org/10.1016/j.egypro.2012.01.136

[7] Yang, S., Yi, P. and Habchi, C. (2020) Real-Fluid Injection Modeling and LES Simulation of the ECN Spray A Injector Using a Fully Compressible Two-Phase Flow Approach. *International Journal of Multiphase Flow*, **122**, 103145. https://doi.org/10.1016/j.ijmultiphaseflow.2019.103145

[8] Troshko, A.A. and Hassan, Y.A. (2001) A Two-Equation Turbulence Model of Turbulent Bubbly Flow. *International Journal of Multiphase Flow*, **27**, 1965-2000. https://doi.org/10.1016/S0301-9322(01)00043-X

[9] De Lorenzo, M., Lafon, P., Pelanti, M., Pantano, A., Di Matteo, M., Bartosiewicz, Y. and Seynhaeve, J.-M. (2021) A Hyperbolic Phase-Transition Model Coupled to Tabulated EoS for Two-Phase Flows in Fast Depressurizations. *Nuclear Engineering and Design*, **371**, 110954. https://doi.org/10.1016/j.nucengdes.2020.110954

[10] Roth, G.A. and Aydogan, F. (2015) Derivation of New Mass, Momentum, and Energy Conservation Equations for Two-Phase Flows. *Progress in Nuclear Energy*, **80**, 90-101. https://doi.org/10.1016/j.pnucene.2014.12.007

[11] Yadigaroglu, G. and Lahey Jr, R. (1976) On the Various Forms of the Conservation Equations in Two-Phase Flow. *International Journal of Multiphase Flow*, **2**, 477-494. https://doi.org/10.1016/0301-9322(76)90011-2

[12] Krepper, E., Končar, B. and Egorov, Y. (2007) CFD Modelling of Subcooled Boiling—Concept, Validation and Application to Fuel Assembly Design. *Nuclear Engineering and Design*, **237**, 716-731. https://doi.org/10.1016/j.nucengdes.2006.10.023

[13] Abraham, J., Sparrow, E. and Minkowycz, W. (2011) Internal-Flow Nusselt Numbers for the Low-Reynolds-Number End of the Laminar-to-Turbulent Transition Regime. *International Journal of Heat and Mass Transfer*, **54**, 584-588. https://doi.org/10.1016/j.ijheatmasstransfer.2010.09.012

[14] Adams, T., Abdel-Khalik, S., Jeter, S. and Qureshi, Z. (1998) An Experimental Investigation of Single-Phase Forced Convection in Microchannels. *International Journal of Heat and Mass Transfer*, **41**, 851-857. https://doi.org/10.1016/S0017-9310(97)00180-4

[15] Taler, D. and Taler, J. (2017) Simple Heat Transfer Correlations for Turbulent Tube Flow. E3S Web of Conferences 13, 02008.

https://doi.org/10.1051/e3sconf/20171302008

[16] Brown, G.O. (2003) The History of the Darcy-Weisbach Equation for Pipe Flow Resistance. *Environmental and Water Resources History*, American Society of Civil Engineers, pp. 34-43. https://doi.org/10.1061/40650(2003)4